

# Multiple Transmission–Reflection Infrared Spectroscopy for High-Sensitivity Measurement of Molecular Monolayers on Silicon Surfaces

Hong-Bo Liu,<sup>†</sup> Nagaiyanallur V. Venkataraman,<sup>‡</sup> Tobias E. Bauert,<sup>‡</sup> Marcus Textor,<sup>‡</sup> and Shou-Jun Xiao<sup>\*,†</sup>

State Key Laboratory of Coordination Chemistry, School of Chemistry and Chemical Engineering, Nanjing National Laboratory of Microstructures, Nanjing University, Nanjing 210093, China, and Laboratory for Surface Science and Technology, Department of Materials, ETH Zurich, Wolfgang-Pauli-Strasse 10, CH-8093 Zurich, Switzerland

Received: May 22, 2008; Revised Manuscript Received: August 28, 2008

A new infrared spectroscopic measurement involving multiple transmissions and reflections for molecular monolayers adsorbed on silicon surfaces has been established. Compared to the well-known multiple internal reflection (MIR) method, the distinctive advantage of multiple transmission-reflection infrared spectroscopy (MTR-IR) is the convenient measurement using standard silicon wafers as samples, while in the MIR setup special fabrication of geometric shapes such as 45° bevel cuts on an attenuated total reflection silicon crystal is needed. Both p- and s-polarized spectra can be obtained reproducibly with the same order of sensitivity as by the MIR spectroscopy. Optimal conditions for spectral acquisition have been obtained from theoretical calculations. The ability of this methodology to gather high quality infrared spectra of adsorbed monolayers is demonstrated and the analysis of the surface packing and molecular orientation is discussed.

## Introduction

Infrared reflection–absorption spectroscopy (IRRAS) has been used widely for its powerful and nondestructive illumination of structure, quality, and orientation of molecular monolayers adsorbed on metallic surfaces.<sup>1</sup> Unfortunately, the characterization of the monolayer on silicon surfaces requires special attention. Unlike on metals, external reflection with p-polarized incident light does not yield enough reflection signals because the Brewster angle of air/silicon interface (73.6°) is close to the grazing angle, allowing most of the light passes through the silicon wafer and escape from the detector. Furthermore, for monolayers, at certain tilt angles, the absorbance might be zero because of the cancelation of parallel and perpendicular components in p polarization.<sup>2</sup> Normal transmission is not sensitive enough for monolayers because of the fewer molecules detected and most of light being reflected. Transmission with p-polarized light at the Brewster angle is by far the simplest way to detect monolayers on silicon because all of the p-polarized light passes through the silicon wafer and reaches the detector.<sup>3</sup> However, the sensitivity of the single transmission, especially for monolayer samples, is still not high enough to allow quantitative analysis. The most popular way for detection of silicon based monolayers is multiple internal reflection (MIR),<sup>4</sup> in which the monolayer is fabricated on an attenuated total reflection (ATR) silicon crystal with 45° bevel cuts at both ends, and the sensitivity is increased by multiple reflections. This technique can provide excellent spectra for molecular monolayers, but the costly ATR crystal restricts its use as a routine laboratory method. It has to be carefully recycled for subsequent use, and the monolayer/silicon interface cannot be used for further device-fabrication. Recently, a germanium (Ge)

ATR measurement was developed by directing the IR beam through a higher refractive index ATR crystal, Ge, to a sample monolayer supported by another higher refractive index Si material (briefly as Ge/monolayer/Si) at an incident angle larger than the critical angle (65° for the Ge/Si interface) to ensure a total reflection.<sup>5</sup> The signal enhancement up to 30 times was reported for perfect optical contact between the incidence phase and the sample.<sup>5d</sup> Since the spectra of sandwiched sample layers strictly follow the surface selection rule, where only the perpendicular vibration modes are enhanced, the molecular orientation can be deduced from the relative intensities of different vibrational modes.<sup>5e</sup> Takoudis et al. and we have individually reported a method, grazing angle mirror-backed reflection (GMBR), for IR analysis of ultrathin SiO<sub>2</sub> films<sup>6a</sup> and silicon-based organic monolayers,<sup>6b</sup> respectively, by placing a mirror behind the double-side-polished silicon wafer in the grazing angle external reflection experiment. The absorbance was reported to be enhanced 6 times as that by the grazing angle external reflection<sup>6a</sup> and 2–3 times as that by transmission at the Brewster angle.<sup>6b</sup> But the sensitivity is still not high enough for molecules with weak absorption and subsequently the weak signal affects the accuracy of quantitative analysis. On the basis of GMBR, we establish a multiple transmission-reflection (MTR) method for characterization of silicon-based organic monolayers by placing the sample between two parallel gold mirrors. When light reaches the silicon surface, it will be split into transmitted and reflected parts leading to multiple transmissions and reflections between two mirrors (Figure 1). The absorbance of monolayers on silicon surfaces will, therefore, be enhanced much higher than by GMBR. A pioneering work on ultrathin soft material films coated on a metal surface using two parallel metal mirrors was carried out by R. G. Greenler.<sup>1b</sup> This configuration was used by V. P. Tolstoy et al. about 20 years ago for detection of an ultrathin SiO<sub>2</sub> layer on silicon wafer inserted between two metal mirrors with p-polarized light at the Brewster incident angle.<sup>7</sup> Unfortunately, further develop-

\* To whom correspondence should be addressed. Fax: 86 25 83314502. Phone: 86 25 83595706. E-mail: sjxiao@nju.edu.cn.

<sup>†</sup> Nanjing University.

<sup>‡</sup> Laboratory for Surface Science and Technology, Department of Materials.

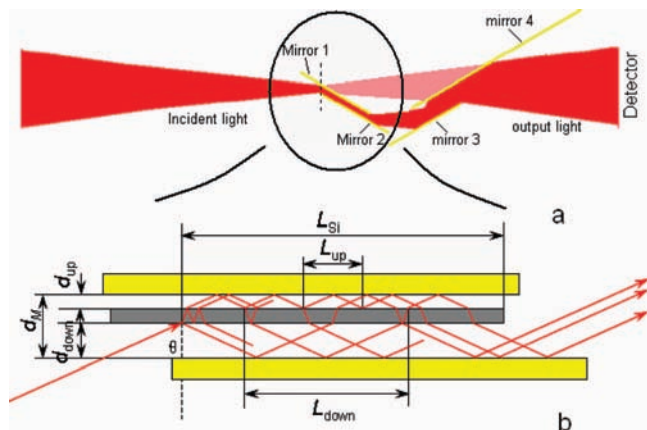


**Figure 1.** (a) Scheme of the MTR setup. The incident light from the interferometer, after multiple transmissions and reflections on the silicon wafer placed between gold mirrors 1 and 2, is guided to the detector by mirrors 3 and 4. The red part denotes the infrared light going through the accessory, and the pink one is the original light path of instrument. (b) Detailed view of the sampling mirrors and the parameters used in the calculation. The effective length of silicon wafer ( $L_{Si}$ ) is the distance from the incident spot to the other end of the wafer.  $L_{up}$  and  $L_{down}$  are the periodic horizontal lengths in the upper and in the lower media respectively, defined by the distance on the upper face of the silicon after a single reflection on the gold surface.  $d_M$  is the mirror distance, and  $d_{up}$  and  $d_{down}$  are the thicknesses of air gaps respectively.

ment of this configuration for the characterization of organo- and biomolecular monolayers on the silicon surface has not been investigated yet, especially considering their wide range of applications in molecular- and nanoelectronics and in biointerfaces. Here, we show that this geometry is powerful for detection of monolayers on silicon surfaces. Theoretical calculation demonstrates that the sensitivity of MTR can be comparable to MIR. The most important advantage of MTR measurement, worth of special attention, is the replacement of the expensive ATR crystal with the ordinary double-side-polished silicon wafer. With optimized parameters, both p- and s-polarized spectra can be firmly obtained, from which further information regarding the orientation of molecules can be deduced from dichroic ratios.<sup>4d,e</sup>

## Experimental Details

**Sample Preparation.** Double-side-polished and (111) oriented p-type silicon wafers (B doped,  $\sim 15 \Omega\text{cm}$  resistivity and 0.5 mm thick, from Si-Mat, Germany) were cut into rectangular shapes ( $18 \times 30 \text{ mm}^2$ ) for infrared analysis. Gold mirrors were prepared by thermal evaporation of a 150-nm Au layer onto a single-side-polished silicon coated with a 10-nm Cr adhesion layer. Si wafers were sonicated for 10 min in toluene and ethanol and then cleaned with “piranha solution” (3:1 (v/v) concentrated  $\text{H}_2\text{SO}_4/30\% \text{H}_2\text{O}_2$ ) for 30 min (Caution: piranha solution reacts violently with organic materials and should be handled with great care), followed by thorough rinsing with Milli Q water (18  $\text{M}\Omega/\text{cm} \text{H}_2\text{O}$ ) and dried under a stream of nitrogen. Octadecyltrichlorosilane (OTS, 97%) and decyltrichlorosilane (DTS, 97%) were purchased from Aldrich. High-performance liquid chromatography grade toluene was purchased from Acros Organics. Silanization was performed in a sealed glass bottle for 2 h at room temperature by inserting the wafer into a fresh solution of 1 mM OTS in toluene, followed by rinsing with toluene, chloroform, and ethanol to remove the physisorbed silanes. Preparation of H-terminated silicon surfaces and further undecylenic acid (UA) monolayers and *N*-hydroxy succinamide

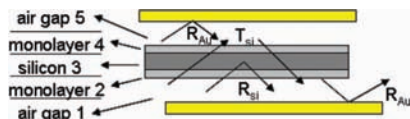


**Figure 2.** Simplified five layer media in the MTR configuration for the simulation.  $T_{Si}$  and  $R_{Si}$  are the transmittance and reflectance of (monolayer)/Si/(monolayer), respectively.  $R_{Au}$  is the reflectance of gold surface.<sup>6b</sup>

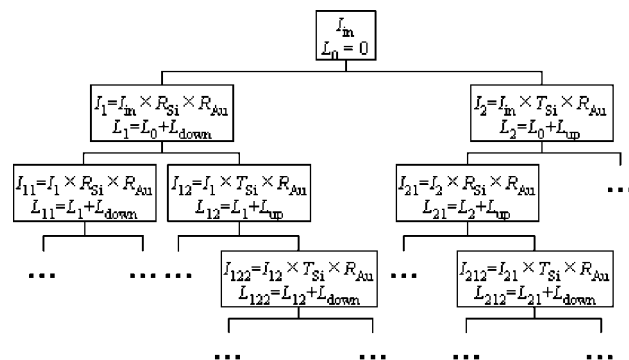


**Figure 3.** Flowchart for the calculation of accumulative total intensities ( $I_{0,out}$  and  $I_{out}$ ) of the output light in the MTR configuration.  $I_{in}$  is the intensity of the incident light.  $R_{Si}$  and  $T_{Si}$  are the reflectance and transmittance of (monolayer)/Si/(monolayer), respectively. The intensity in each branch is obtained by multiplying with  $R_{Si}$  and  $T_{Si}$  for reflection and transmission at the (monolayer)/Si/(monolayer) interface, respectively, and with  $R_{Au}$  for reflection on the gold mirror. The subscripts indicate accumulative reflections and transmissions at the (monolayer)/Si/(monolayer) interface, where 1 and 2 represent one reflection and one transmission, respectively.

(NHS) functionalized monolayers were performed as described in our earlier reports.<sup>6b</sup> Infrared spectra were recorded on a Bruker IFS66/S instrument at  $4\text{-cm}^{-1}$  resolution. A grid polarizer was installed in the light path between the source and the sample. A double side polished silicon wafer pre-cleaned with piranha solution was used as background. Unless specified, a DTGS detector and a scan time of 3 min were used for measurements.

**MTR Set Up.** A schematic of the MTR setup and the optical geometry is shown in Figure 1. It is composed of four mirrors; two of them are sampling mirrors (mirror 1 and 2), and the other two are the guiding mirrors (mirrors 3 and 4) to redirect the beam onto the detector. The sample, silicon wafer, is inserted between the two sampling mirrors, with one end protruding out at about 5 mm of the incident spot, in order to make sure that the first reflection is on the silicon surface. The distance between the silicon wafer and two sampling mirrors can be adjusted with two micrometers. The two guiding mirrors can be moved back and forth to get the maximal amplitude. The incident angle was controlled by two step-motors with a minimal angle of  $0.225^\circ$ .

**Simulation Details. Absorbance and Absorption Depth ( $A$  and  $\Delta R$ ).** The MTR configuration can be simplified as five layers for the simulation, as shown in Figure 2: two air gaps (1 and 5), two monolayers (2 and 4), and silicon (3). The reflectance ( $R_{Si}$ ) and transmittance ( $T_{Si}$ ) at each time when the infrared beam interacts with the sample, (monolayer)/Si/(monolayer), are obtained, considering the silicon wafer as an incoherent thick film between two semi-infinite air media, according to the equations we used previously.<sup>6b</sup> And then the three layers, (monolayer)/Si/(monolayer), are treated as a single interface during further calculations to get the final intensity of the output light.

The step-by-step calculations to obtain the accumulative total intensities of the output light ( $I_{0,out}$  and  $I_{out}$ ) is illustrated in Figure 3. When light reaches the sample interface, (monolayer)/

Si/(monolayer), it is split into reflection and transmission components, and both return to this interface again after reflection on gold surfaces. This process defines a periodic horizontal length passed by the light in the upper ( $L_{up}$ ) and the lower media ( $L_{down}$ ) in Figure 1. The split light intensity is multiplied with  $T_{Si}$ ,  $R_{Si}$ , or  $R_{Au}$  (reflectance on gold surface), respectively, each time when the light meets these interfaces. Simultaneously, after each step, the horizontal length of light passed was added with  $L_{down}$  or  $L_{up}$ , respectively (Figure 3). This calculation was continued until  $L$  is larger than the effective length of silicon wafer ( $L_{Si}$ ) or the intensity is less than  $I_0 \times 10^{-4}$ . The sum of all terminal intensities of each branch in Figure 3 was the accumulative total intensity of the output light. The absorbance  $A$  and the absorption depth  $\Delta R$  were obtained using the simple relations

$$A = -\log_{10} \left( \frac{I_{out}}{I_{0,out}} \right) \quad (1)$$

$$\Delta R = \frac{I_{0,out}}{I_{in}} - \frac{I_{out}}{I_{in}} \quad (2)$$

**Orientation Analysis.** For orientation analysis of a self-assembled octadecyl trichlorosilane (OTS) monolayer on silicon, a uniaxial symmetry of the alkyl chain was considered, which means that the azimuth angle and the twist angle are not defined. The tilt angle  $\gamma$  of the alkyl chain with the surface normal can be related to the anisotropic absorption index  $k$ , where  $k$  is the imaginary part of the complex refractive index ( $\hat{n} = n + ik$ ) from the following equations<sup>8</sup>

$$k_x = k_y = k_{max} [s(\sin^2 \alpha)/2 + (1-s)/3] \quad (3)$$

$$k_z = k_{max} [s(\cos^2 \alpha) + (1-s)/3] \quad (4)$$

$$s \equiv \langle p_2 \cos \gamma \rangle = \frac{1}{2} \langle 3 \cos^2 \gamma - 1 \rangle \quad (5)$$

where  $s$  is the long-axis order parameter,  $k_{max}$  is the absorption index along the transition dipole moment (TDM),  $k_z$  is the perpendicular component of absorption index to the surface, and  $k_x$  and  $k_y$  are the parallel components, and  $\alpha$  is the angle between TDM and the long molecular axis. For a special case, the all-trans alkyl chain, the TDMs of both symmetric and asymmetric methylene stretching vibrations are perpendicular to the carbon backbone, and thus  $\alpha = 90^\circ$ . We use the DR (dichroic ratio) fitting method, which is well accepted in MIR, to calculate the tilt angle  $\gamma$  of the molecular monolayer. Theoretically,  $A_s$  and  $A_p$ , and thus the dichroic ratio ( $DR = A_s/A_p$ ) are calculated from the anisotropic  $R_{Si}$  and  $T_{Si}$ , which are related to  $\gamma$ -dependent anisotropic complex refractive index ( $\hat{n}_j = n + ik_j$ , where  $j = x, y$ , and  $z$ ) in our previous publication.<sup>6b</sup> Thus, a curve of DR vs tilt angle  $\gamma$  can be simulated for a fixed  $k_{max}$  and the experimental dichroic ratio ( $DR = A_s/A_p$ ), obtained from the s- and p-polarized MTR spectra, can be used to obtain the tilt angle  $\gamma$ .

**Influence of Absorbance and Absorption Depth by Parameters.** The MTR spectra are affected by several parameters, the most important among them being the incident angle ( $\theta$ ) and the distances between two mirrors ( $d_M$ ) and between silicon and upper and down mirrors ( $d_{up}$  and  $d_{down}$ ) respectively, and the effective length of silicon wafer ( $L_{Si}$ ). Since the number of reflections and transmissions through the silicon wafer changes when these parameters are perturbed, the absorbance and the signal-to-noise ratio (SNR) will be influenced. The band intensity is determined by the absorbance, and SNR is proportional to the absorption depth in a noise-limited spectrometer.<sup>7b</sup>

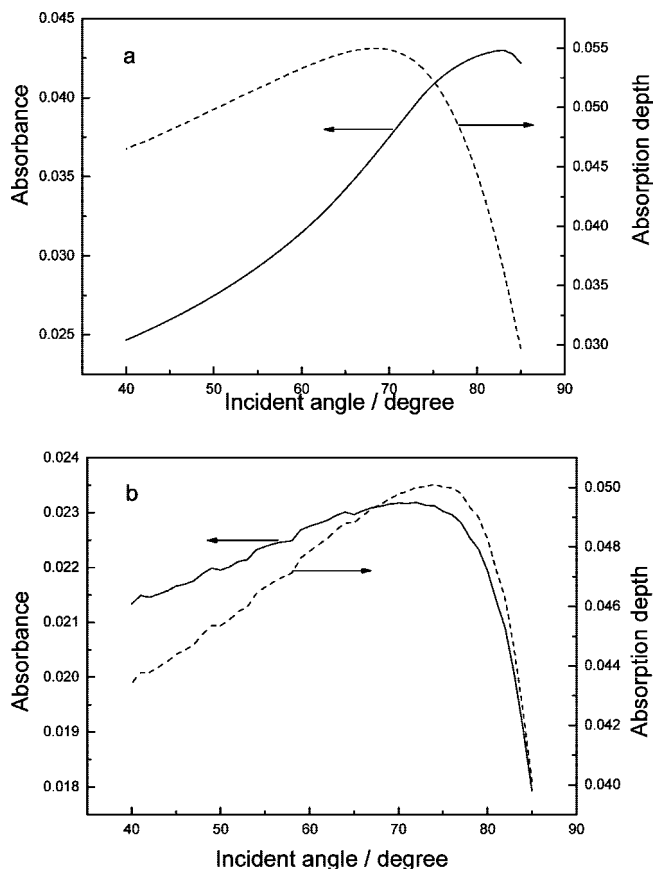


**Figure 4.** Calculated absorbance ( $A$ , solid line) and absorption depth ( $\Delta R$ , dashed line) vs incident angle for a 2.6 nm isotropic hydrocarbon adlayer ( $n = 1.5$ ,  $k = 0.5$ ) in (a) p polarization and (b) s polarization at  $2918 \text{ cm}^{-1}$ . MTR parameters for calculation are  $N = 8$ ,  $d_{up} = 0.05 \text{ mm}$ , and  $L_{Si} = 25 \text{ mm}$ .

Simulation analysis will provide optimum parameters for measuring high quality spectra. We define the number of simplified transmission times ( $N$ ) as number of times the beam passes through the silicon until it leaves for the guiding mirror, assuming no reflection on the silicon surface. However during our simulation process, we account for all transmissions and reflections on silicon and reflections on gold surfaces, as shown in Figure 3. The number of simplified transmission times ( $N$ ) is just a parameter for simplicity and clarity to depict the complex process of reflection-transmission used in the calculation.

First we consider the effect of the incident angle on the sensitivity of measurements. The goal is to figure out the optimal incident angle for obtaining both high absorbance and SNR at the same time. Figure 4 shows the curves of absorbance and absorption depth drawn against incident angle for p and s polarizations, where  $N$  is fixed to 8. The calculations have been done for an isotropic hydrocarbon layer at  $2918 \text{ cm}^{-1}$  with typical optical constants of  $n = 1.5$  and  $k = 0.5$ . The angular dependence of absorbance for p polarization exhibits the maximum around  $80^\circ$ , but the absorption depth goes down steeply after  $74^\circ$ . For s polarization, both absorbance and absorption depth shows maximum between  $70^\circ$ – $74^\circ$ . This similarity of maximum absorbance and absorption depth of both p and s polarizations facilitates the choice of the optimal angle of incidence to be between  $70^\circ$ – $74^\circ$  in our measurements.

We now fix the angle of incidence at  $74^\circ$  to study the effect of the number of simplified transmission times ( $N$ ) on the sensitivity. The distance between the two sampling mirrors and the size of the silicon sample determines the number of

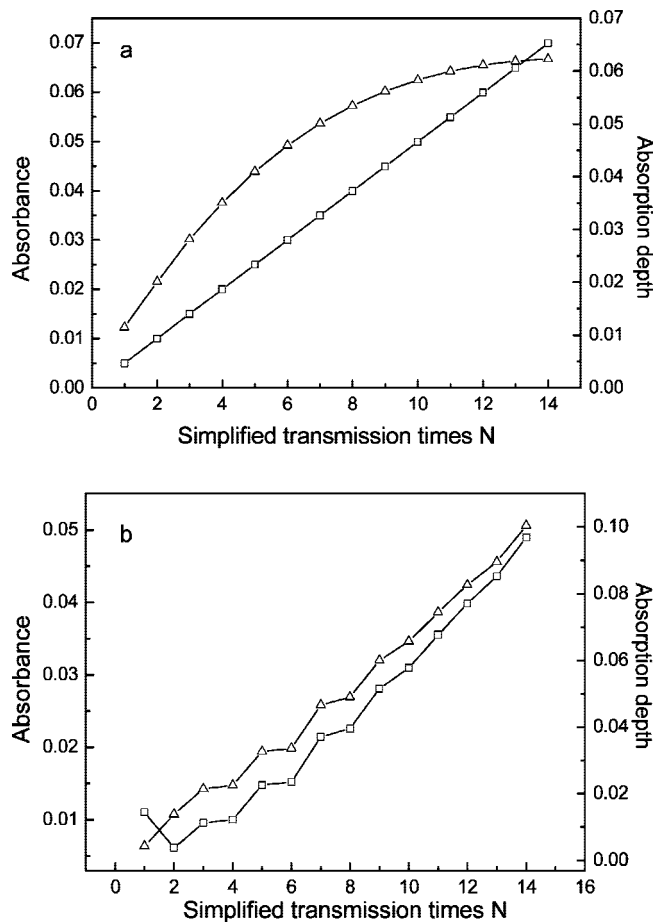


**Figure 5.** Calculated absorbance ( $A$ ,  $\square$ ) and absorption depth ( $\Delta R$ ,  $\triangle$ ) vs simplified transmission times ( $N$ ) for a 2.6-nm layer ( $n = 1.5$ ,  $k = 0.5$ ) at  $2918\text{ cm}^{-1}$  in (a) p polarization and (b) s polarization at an incident angle of  $74^\circ$ . The mirror distance  $d_M$  between two gold mirrors is changed with different transmission times, while  $d_{\text{up}}$  is fixed at 0.3 mm.

transmission-reflection times and consequently the sensitivity of this measurement. The values of  $N$  used in the calculation have been limited to a narrow range, 1–14, considering the unreasonably larger silicon sample size and the unrealistic smaller mirror distances that would be required to achieve larger values of  $N$  in a practical experiment. The absorbance and the absorption depth calculated for different values of  $N$  are plotted in Figure 5. The absorbance of p polarization goes up proportionally to  $N$ . This can be expected since no loss in intensity occurs for p polarization at an incident angle close to the Brewster angle of air/silicon ( $73.6^\circ$ ). Therefore it is equivalent to measuring a stack of  $N$  identical samples in parallel. While this is true for the absorbance, the calculated absorption depth increases steeply only up to a value of  $N$  smaller than 6 and then begins to saturate at higher numbers of  $N$  (Figure 5a). The limitation of the absorption depth of p polarization is due to the decrease of output intensity with increasing  $N$ , similar to that has been shown for multiple reflections between two metallic surfaces.<sup>1b</sup> Because we consider Si being transparent in all calculations, the only energy loss comes from the reflection on gold mirrors. The complex refractive index of gold is  $2.018 + 21.087i$  at  $2918\text{ cm}^{-1}$ ,<sup>9</sup> and the corresponding reflectance is 0.9397 and 0.9950 for p and s polarizations, respectively. For s polarization, where the light has a high reflectance on gold surfaces, both absorbance and absorption depth increase with increasing  $N$  (Figure 5b) with the exception of  $N = 2$ . As shown in Figure 5b, the absorbance

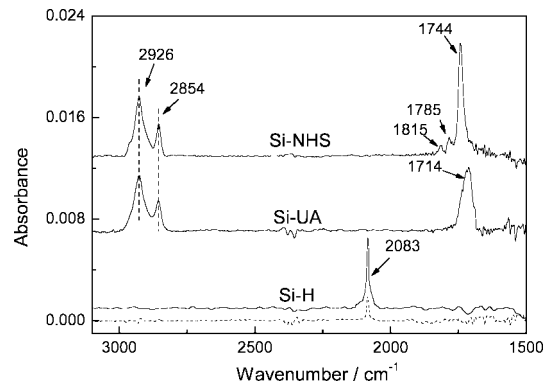


**Figure 6.** Experimental p-polarized spectra of Si–H and UA and NHS ester monolayers measured with the MTR methodology. The spectra were measured with  $d = 2.0$  mm and an incident angle of  $74^\circ$ . The region of  $2400\text{--}2280\text{ cm}^{-1}$  is the absorption disturbance of  $\text{CO}_2$  and of  $1500\text{--}1800\text{ cm}^{-1}$  is due to  $\text{H}_2\text{O}$ . Spectra are shown after baseline correction and subtraction of water and  $\text{CO}_2$ .

at  $N = 2$  is lower than that of the single transmission, which means that the MTR measurement for s polarization, unlike the p polarization, is a combination of transmission and reflection components, due to its high reflectance on air/silicon at the Brewster incident angle ( $R_{\text{Si}}$  is around  $0.83^{10}$ ). However, if the above calculation only includes the reflections between a silicon and a gold mirror, the absorption depth would be very low, compared to the MTR measurement, especially at high reflection times (see Section 1 in Supporting Information).

It is evident from the data presented in Figures 4 and 5 that the MTR measurement is a unique combination of transmission and reflection. The above theoretical consideration, taken together with the practical limitation for the silicon wafer size and the precise control of mirror distances, has led to a set of optimal conditions for spectra acquisition:  $N = 6$ ,  $d_M = 2$  mm,  $d_{\text{up}} = 0.3$  mm,  $L_{\text{Si}} = 25$  mm, and an incident angle of  $74^\circ$ . All the experimental spectra discussed below were recorded with these optimized parameters. The high-quality infrared spectra of adsorbed monolayers by MTR are demonstrated on H-terminated silicon derivatized monolayers and on long alkyl chain silanized monolayers, followed by a detailed discussion of the orientation of alkyl chains on silane monolayers.

## Results and Discussions

**MTR Spectra of Hydrogen-, Undecylenic Acid-, and NHS-Terminated Surfaces.** Spectra measured with p polarization on H-terminated, undecylenic acid (UA) and its further derivatized NHS ester monolayers on silicon surfaces are shown in Figure 6. The peak at  $2083\text{ cm}^{-1}$  is typical for the monohydrogen-terminated Si(111) surface. Upon the reaction with the end double bond ( $\text{C}=\text{C}$ ) of UA, this peak disappears completely, while a new set of bands appear at  $2926$  and  $2854\text{ cm}^{-1}$ , for  $\nu_{\text{as}}\text{CH}_2$  and  $\nu_{\text{s}}\text{CH}_2$ , respectively, and at  $1714\text{ cm}^{-1}$ , for the  $\text{C}=\text{O}$  stretching band of carboxylic acid group. After further functionalization with NHS, the specifically coordinated three peaks ( $1815$ ,  $1785$ , and  $1744\text{ cm}^{-1}$ ), assigned to succinimidy ester, are clearly shown. The assignments of the bands are similar to those reported in our earlier publication using GMBR.<sup>6b</sup> For comparison, we have also included the spectrum of H-terminated silicon in Figure 6 (bottom trace) measured by GMBR. Obviously, a substantial improvement in the spectral signal and SNR is observed for the same monolayer on silicon. The higher sensitivity of the MTR methodology to study the surface species on a silicon surface compared to GMBR is clearly demonstrated.

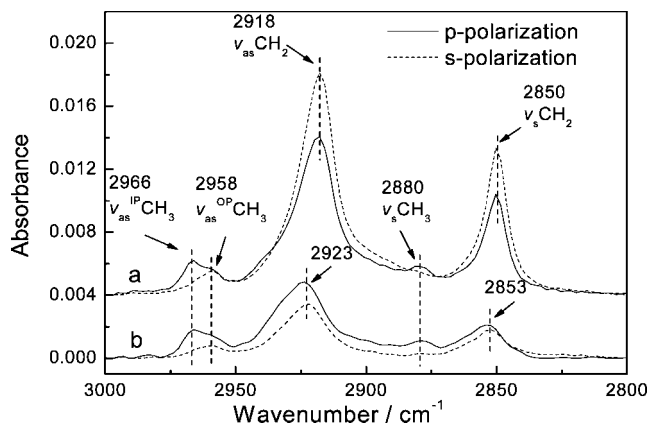


**Figure 7.** Experimental spectra of (a) OTS and (b) DTS monolayers with MTR for p (solid line) and s (dashed line) polarization. The incident angle is  $74^\circ$ , and the mirror distance is 2.0 mm.

However, the real advantage of MTR over GMBR and Ge/monolayer/Si lies in its ability to measure the spectra of adsorbed layers with high sensitivity in both s and p polarizations, which can be used to infer information concerning the orientation of the adsorbed species. The UA and NHS monolayers are not suitable for orientation analysis due to their disordered chain structures as indicated by the C–H stretching bands (Figure 6) discussed in our previous publication.<sup>6b</sup> To demonstrate the feasibility of MTR for molecular orientations, we used the well-known self-assembled monolayers of OTS and decyl trichlorosilane (DTS) on the commercial silicon wafer surface with an ultrathin  $\text{SiO}_2$  passivation layer. Long chain alkylsilanes are known to form highly organized compact monolayers on silicon surfaces.

**Orientation Analysis of OTS and DTS.** Spectra of OTS and DTS monolayers with p and s polarizations in the C–H stretching region are given in Figure 7 (the whole spectra in  $4000\text{--}1500\text{ cm}^{-1}$  region are given in Supporting Information, Section 5). The positions of methylene stretching vibrations are sensitive to the molecular order. The peaks of  $\nu_{\text{as}}(\text{CH}_2)$  and  $\nu_{\text{s}}(\text{CH}_2)$  shift from 2918 and  $2850\text{ cm}^{-1}$  to 2923 and  $2853\text{ cm}^{-1}$ , respectively, from OTS to DTS, but no shift of the wavenumber of any stretching mode of  $\text{CH}_3$  is observed, which indicates a disordered gauche structure in the DTS monolayer.<sup>7b</sup> On the silicon surface, both normal (z) and parallel (x) components of transition dipole moment (TDM) contribute to the absorption for p polarization, while only the parallel (y) component contributes for s polarization. This is evident from the spectra wherein both in-plane ( $2966\text{ cm}^{-1}$ ) and out-of-plane ( $2958\text{ cm}^{-1}$ ) modes of  $\nu_{\text{as}}(\text{CH}_3)$  can be seen in p-polarized spectra, while only the out-of-plane mode is clearly visible in s polarization. By assumption of an extended all-trans conformation of the alkyl chains, the TDMs of the methylene stretching modes are perpendicular to the alkyl chain. The stronger intensity of the methylene stretching modes in the OTS s-polarized spectrum indicates that its alkyl chain is closer to the normal of the surface than that of DTS.

Generally, the major problem in orientation analysis is the determination of both thickness and absorption index of TDM ( $k_{\text{max}}$ ). Although usually the layer thickness can be detected by ellipsometry and  $k_{\text{max}}$  could be obtained from the isotropic constant using the relationship  $k_{\text{max}} = 3.0k_{\text{iso}}$  assuming a perfect orientation of all TDMs, there are still errors in measurement of the thickness in the nanometer scale, and  $k_{\text{max}}$  is a function of the molecular packing and orientation.<sup>8</sup> Compared to the “spectrum fitting” method<sup>2,11</sup> for determination of molecular

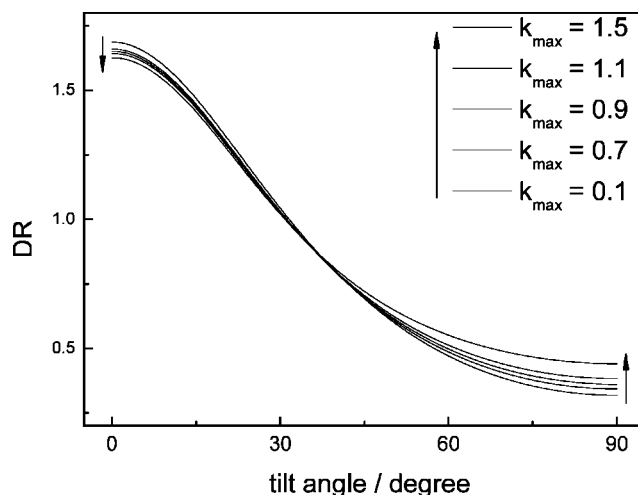


**Figure 8.** The effect of absorption index  $k_{\text{max}}$  (0.1, 0.7, 0.9, 1.1, 1.5) calculated with refractive index of 1.5 on DR/tilt-angle curves for MTR measurements for a 2.6-nm layer at  $2918\text{ cm}^{-1}$ . In calculation, the incident angle is  $74^\circ$ ,  $d_{\text{up}} = 0.3\text{ mm}$ , and  $L_{\text{Si}} = 25\text{ mm}$ . A beam divergence of  $7.5^\circ$  and a diameter of the focused spot of 6 mm were considered in the calculations.

orientations, the “DR fitting”<sup>4d,e</sup> approach is less dependent on the accuracy of these values. However, “DR fitting” depends highly on the quality of both s- and p-polarized spectra to obtain reliable dichroic ratios. Therefore, this approach thus far has been mainly restricted to the MIR measurement due to the high SNR. Since our MTR method provides nearly the same quality spectra as by MIR in both p and s polarizations, reliable DR values can be obtained and used for the analysis of molecular orientations.

The calculated dependence of DR on the tilt angle for  $\text{CH}_2$  at  $2918\text{ cm}^{-1}$  with our MTR configuration is shown in Figure 8. From these “DR fitting” curves, the tilt angle of alkyl chains in an experimental system can be obtained after determining their DR value from spectra. The typical absorption ( $k_{\text{max}}$ ) and refractive ( $n$ ) indices of octadecyl  $\nu_{\text{as}}(\text{CH}_2)$  are 0.9<sup>2</sup> and 1.5,<sup>12</sup> respectively. The experimental DR value for  $\nu_{\text{as}}(\text{CH}_2)$  of OTS at  $2918\text{ cm}^{-1}$  in Figure 7 is 1.42, and it corresponds to a tilt angle of  $15^\circ$  as given by Figure 8. The DR value for  $\nu_{\text{as}}(\text{CH}_2)$  of DTS is about 0.73, much lower than the value of OTS, and it corresponds to an average tilt angle of about  $43^\circ$ . But this value is physically less meaningful because of the disordered gauche conformation of the alkyl chains in DTS monolayers.

However, it has been argued that the values of  $k_{\text{max}}$  could change when a molecule is chemisorbed on surfaces.<sup>8</sup> To investigate the error of tilt angle induced by the inaccuracy of  $k_{\text{max}}$  in our “DR fitting” approach, five  $k_{\text{max}}$  (= 0.1, 0.7, 0.9, 1.1, and 1.5) values covering all possibilities are plotted in Figure 8. The five curves converge at a tilt angle of  $36^\circ$ , indicating that around this value the influence of  $k_{\text{max}}$  on DR and therefore on the tilt angle, can be ignored. Even in the wide range of  $k_{\text{max}}$  from 0.1 to 1.5, the resulting tilt angle of the OTS monolayer has an error of only about  $\pm 2^\circ$ . If  $k_{\text{max}}$  can be known more precisely from the isotropic absorption index to a narrower range of 0.7–1.1,<sup>2,8</sup> this error will be further reduced to  $\pm 0.5^\circ$ .

Apart from the optical constants, the inaccuracy of some parameters used in the MTR configuration, including the mirror distances and the effective length of silicon samples, will result in errors in the calculation of tilt angles (see Sections 3, 4, and 5 in Supporting Information). By consideration of all the effects mentioned above, the tilt angle of the OTS alkyl chain in our experimental system is estimated as  $15 \pm 3^\circ$ , which is close to the reported value.<sup>13</sup>

## Conclusions

We have investigated in detail a MTR methodology to obtain high-quality infrared spectra of molecular monolayers adsorbed on silicon surfaces. The method is based on allowing multiple transmissions and reflections to occur on a silicon surface by placing a double-side-polished silicon sample between two parallel gold mirrors within a distance of 2 mm. Optimal conditions for spectral acquisition such as the number of transmission–reflections, incident angle, and mirror distance are chosen from theoretical calculations. Our experiments confirm that the MTR method can reach the same high-sensitivity and high-quality spectra as that of the most commonly used MIR and the recently developed Ge/monolayer/Si methods. MTR provides a convenient noncontact and nondestructive measurement of derivatized molecular monolayers on commercial silicon wafers. Moreover because of the nondestructive nature of MTR, the quality-controlled samples can be used for further device fabrications. The combination of transmissions and reflections gives rise to high enough absorbance and SNR for both p and s polarizations. This allows us to reliably determine the DRs of some vibrational modes for the adsorbed species, hitherto accessible only to the MIR spectroscopy, and thereby their relative orientations to the surface. The optical setup used in this study is designed to adapt to any standard FT-IR spectrometers and further improvements are being pursued. Further, with thin IR-transparent (semitransparent) metal or metal oxide coatings on silicon surfaces, a variety of surface–adsorbate interactions can be studied by the MTR–IR spectroscopy. While MIR will continue to remain as the choice for in situ studies of such interfaces, MTR represents a powerful alternative for ex-situ investigations of surface–adsorbate interactions.

**Acknowledgment.** We are grateful to the financial support of the National Basic Research Program of China, No. 2007CB925101, and NSFC, Nos. 20721002 and 20571042. We thank Prof. Nicholas D. Spencer for his help and suggestions during the work.

**Supporting Information Available:** Numerical analysis of multiple reflections between a single gold mirror and a silicon sample for s-polarization; effect of beam divergence on absorbance; effect of refractive index ( $n$ ) on orientation analysis; effect of mirror distance and effective silicon length on orientation analysis; effect of thickness of air gaps on IR spectra. This material is available free of charge via the Internet at <http://pubs.acs.org>.

## References and Notes

- (1) (a) Greenler, R. G. *J. Chem. Phys.* **1966**, *44*, 310. (b) Greenler, R. G. *J. Chem. Phys.* **1969**, *50*, 1963. (c) Allara, D. L.; Baca, A.; Pryde, C. A. *Macromolecules* **1978**, *11*, 1215.
- (2) Hoffmann, H.; Mayer, U.; Krischanitz, A. *Langmuir* **1995**, *11*, 1304.
- (3) Webb, L. J.; Rivillon, S.; Michalak, D. J.; Chabal, Y. J.; Lewis, N. S. *J. Phys. Chem. B* **2006**, *110*, 7349.
- (4) (a) Harrick, N. J. *Internal Reflection Spectroscopy*; Wiley: New York, 1967. (b) Hamers, R. J.; Hovis, J. S.; Lee, S.; Liu, H.; Shan, J. *J. Phys. Chem.* **1997**, *101*, 1489. (c) Ubara, H.; Imura, T.; Hiraki, A. *Solid State Commun.* **1984**, *50*, 673. (d) Haller, G. L.; Rice, R. W. *J. Phys. Chem.* **1970**, *74*, 4386. (e) Picard, F.; Buffeteau, T.; Desbat, B.; Auger, M.; Pezolet, M. *Biophys. J.* **1999**, *76*, 539.
- (5) (a) Otto, A. *Z. Phys.* **1968**, *216*, 398. (b) Ishino, Y.; Ishida, H. *Appl. Spectrosc.* **1988**, *42*, 1296. (c) Lummerstorfer, T.; Hoffmann, H. *Langmuir* **2004**, *20*, 6542. (d) Lummerstorfer, T.; Hoffmann, H. *Anal. Bioanal. Chem.* **2007**, *388*, 55. (e) Anariba, F.; Viswanathan, U.; Bocian, D. F.; McCreery, R. L. *Anal. Chem.* **2006**, *78*, 3104.
- (6) (a) Cui, Z.; Takoudis, G. C. *J. Appl. Phys.* **2001**, *89*, 5170. (b) Liu, H.-B.; Xiao, S.-J.; Chen, Y.-Q.; Chao, J.; Wang, J.; Wang, Y.; Pan, Y.; You, X.-Z.; Gu, Z.-Z. *J. Phys. Chem. B* **2006**, *110*, 17702.
- (7) (a) Tolstoy, V. P.; Bogdnova, L. P.; Aleskovski, V. B. *Dokl. Doklady USSR* **1986**, *291*, 913. (b) Tolstoy, V. P.; Chernyshova, I. V.; Skryshevsky, V. A. *Handbook of Infrared Spectroscopy of Ultrathin Films*; Wiley-Interscience: New York, 2003.
- (8) Chernyshova, I. V.; Rao, K. H. *J. Phys. Chem. B* **2001**, *105*, 810.
- (9) Barth, J.; Johnson, R. L.; Cardona, M. *Handbook of Optical Constants of Solids II*; Academic Press: New York, 1991.
- (10) Kaplan, S. G.; Hanssen, L. M. *Infrared Phys. Technol.* **2002**, *43*, 389.
- (11) Parikh, A. N.; Allara, D. L. *J. Chem. Phys.* **1992**, *96*, 927.
- (12) (a) Allara, D. L.; Nuzzo, R. G. *Langmuir* **1985**, *1*, 45. (b) Maoz, R.; Sagiv, J. *J. Colloid Interface Sci.* **1984**, *100*, 465. (c) Tillman, N.; Ulman, A.; Schildkraut, J. S.; Penner, T. L. *J. Am. Chem. Soc.* **1988**, *110*, 6136.
- (13) Kojio, K.; Takahara, A.; Omote, K.; Kajiyama, T. *Langmuir* **2000**, *16*, 3932.

JP804553X